Supplementary Information

Nanoscale voxel spectroscopy by simultaneous EELS and EDS tomography

Georg Haberfehlner[a], Angelina Orthacker[a], Mihaela Albu[a], Jiehua Li[b], and Gerald Kothleitner[a,c]

[a]*Graz Centre for Electron Microscopy, Steyrergasse 17, 8010 Graz, Austria*

[b]*Chair of Casting Research, Department of Metallurgy, University of Leoben, Franz-Josef-Strasse 18, 8700 Leoben, Austria*

[b]*Institute for Electron Microscopy and Nanoanalysis, Graz University of Technology, Steyrergasse 17, 8010 Graz, Austria*

S.1. Sample preparation

Samples were prepared from the surface of the AlSi-alloy using an FEI Nova 200 dual-beam focused ion beam (FIB) / scanning electron microscope (SEM). A needle-shaped sample was extracted from the surface of the alloy, attached to an Omniprobe TEM support grid and subsequently ion-milled to reduce its diameter down to 80 nm. Ion milling was done with an acceleration voltage of 30 kV. The diameter of the needle was reduced in several steps, reducing the ion beam current at each step. For the final milling stage the beam current was set to 30 pA. After FIB preparation the sample was transferred to a Fischione 2020 tomography TEM sample holder and plasma cleaned using Ar/O plasma in a Fischione Plasma Cleaner model 1020 for 1 min before the TEM experiments.

S.2. Tilt series acquisition

For analytical electron tomography experiments a probe-corrected FEI Titan^3 G2 60-300 microscope with an X-FEG Schottky field emission electron source operated at 300 kV was used. The electron beam current was set to approximately 1 nA. A convergence semi-angle of 7.5 mrad was used to have larger depth of field. Spectrum images with a size of 194*156 pixel at a pixel size of 1 nm were acquired every 5° from -75° to 80°, with the tilt range being limited by the sample holder. Image acquisition time for each spectrum image was 3 minutes and 20 seconds. EDX spectra and dual-EELS spectra were acquired in parallel using the DigiScan engine in the Gatan Microscopy Suite. EDX spectra were acquired with a pixel time of 10 ms. Dual-EELS spectra were acquired with a collection semi-angle of 19.7 mrad, using a dispersion of 0.5 eV/pixel. Low-loss spectra were acquired with a pixel time of 10 µs over a range of -80 eV to 920 eV and core-loss spectra with a pixel time of 10 ms over a range of 1120 eV to 2060 eV.

S.3. Observation of beam damage and contamination

To estimate whether beam damage and contamination play a significant role in our experiments in Fig. S1a HAADF STEM survey images recorded before and during the tilt series are investigated and Fig. S1b shows EDS spectra summed over the full spectrum images with a focus on the location of the carbon K-line.

In the survey images recorded before and during the tilt series no significant impact of beam damage is visible. In particular areas outside of the region where spectrum images were recorded show no differences in contrast compared to regions inside of this area. Only when the diameter of the sample is investigated in detail it can be seen that in the image acquired during the tilt series the sample diameter in the region of interest appears slightly reduced at some locations, which may have been caused by beam damage. However diameter changes remain small (< 1 nm). Concerning contamination no significant carbon peak is visible at any stage during the experiment, allowing the conclusion that contamination was no serious issue in our experiment.

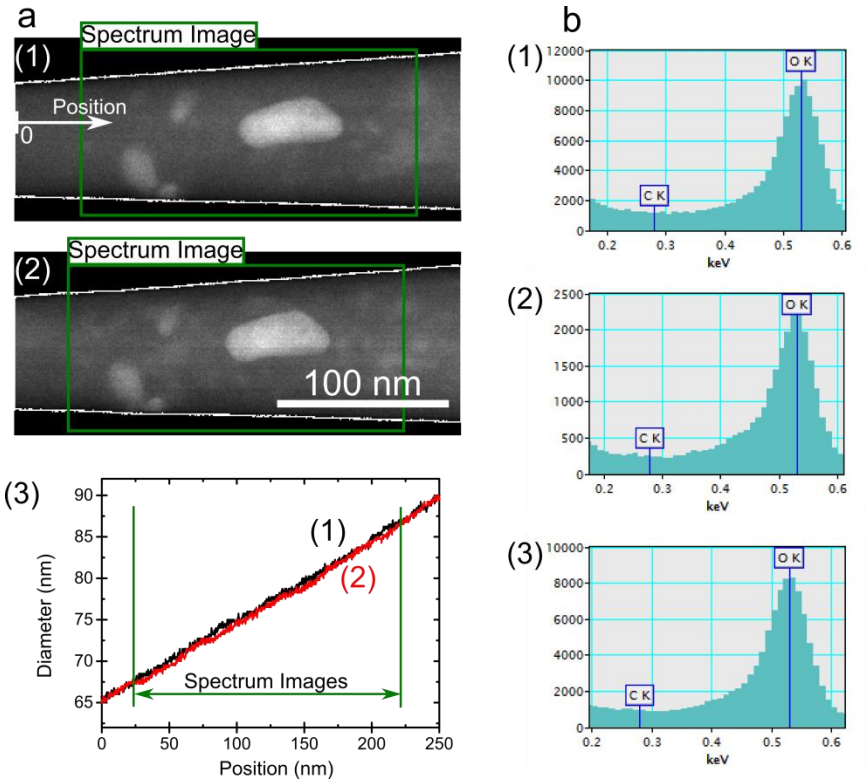

Figure S1: (a) HAADF STEM survey images recorded (1) before acquisition of the tilt series, (2) after half of the tilt series was recorded. Regions where spectrum images are recorded are shown in green. The exterior boundary of the sample is highlighted in white. (3) Measurements of the sample diameter. The black line shows the diameter measured along the sample in (1), the red lines shows the diameter measured in (2). Differences between the two lines could indicate beam damage. (b) Observation of C K-lines in spectra summed over the full spectrum images (1) at the first tilt angle, (2) after half of the tilt series was recorded, (3) at the last tilt angle.

S.4. Principal components analysis

For EELS data processing first of all energy drift correction was done for each spectrum based on the location of the zero-loss peak. For principal components analysis (PCA) the Hyperspy software[1] was used. All acquired core-loss EELS spectra are merged into a single dataset to treat them simultaneously. In PCA the dataset is described by a parametric model of orthogonal components. The problem is assumed to be linear. Components are sorted by their variance and only components with high variance are kept, which should correspond to the signal, while components with a lower variance can be attributed to noise. In our case the large number of spectra (~1 million) provided good statistics for PCA. Based on a scree plot we identified six relevant components, which are kept, while all other components are discarded. Fig. S2a shows the scree plot, Fig. S2b the 6 principal components and Fig. S2c the maps corresponding to the components for the spectrum image at -70°.

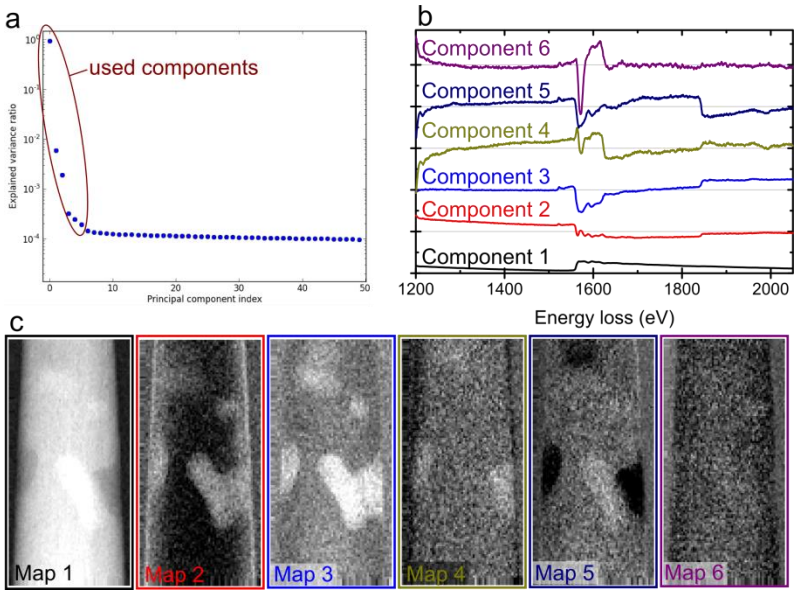

Figure S2: (a) Scree plot showing the ratio of the variance of the first 50 principal components to total variance (b) First 6 components extracted from PCA and (c) corresponding maps for the spectrum image at -70°

S.5. Model-based fitting of EELS spectra

For model-based fitting of the EELS spectra we used two fit regions, a first region starting at 1250 eV up to 1850 eV, a second region starting at 1700 eV up to 1940 eV. The first region contains the Al K-edge and the Yb M_{45}-edge, the second region contains only the Si K-edge and ends just before the Yb M_3-edge. Extracted elemental maps from the Yb M_{45}-edge, the Si K-edge and the Al K-edge for one tilt angle are shown in Fig. S3.

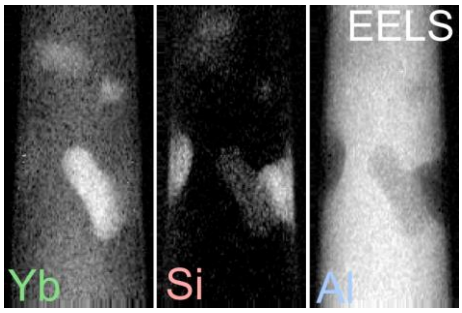

Figure S3: Elemental maps at -70° extracted from EELS data

S.6. Normalization of EDX data

The extracted intensity of the EDX elemental maps strongly depends on the tilt angle (see Fig. S4a&b). This is due to shadowing of x-rays by the sample holder. Depending on the tilt angle parts of the sample holder lie in between the sample and the x-ray detectors thereby lowering the number of counts. To compensate for these shadowing effects we extracted the summed intensity from each elemental map at each tilt angle (see Fig.S4c). The extracted summed intensities were used to normalize the projections. As it can be assumed that the total amount of a specific element should be the same for each tilt angle, we used the summed intensity at each tilt angle for normalizing each projection. These normalized elemental maps were then used as basis for the reconstruction.

Before the reconstruction of the full EDX spectra a similar normalization step as performed for the elemental maps was necessary. We normalized the spectrum images using the sum of the integrated spectral intensity from 1.2 keV to 2 keV. This spectral range contains the Al K-lines, Si K-lines as well as the Yb M-lines and was therefore chosen for the normalization. We note that while a sample holder for needle-shaped supports could help to avoid shadowing effects our method could also be used for samples which cannot be prepared on a needle-shape support.

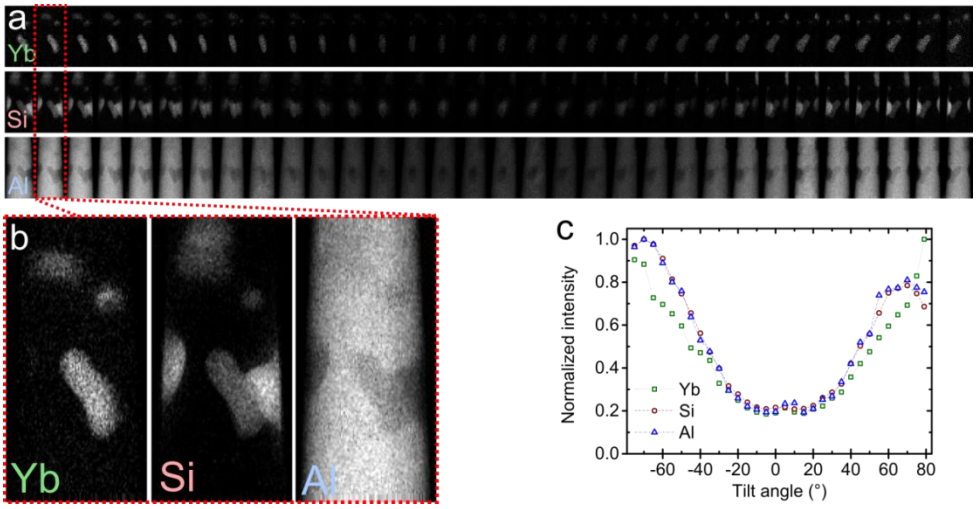

Figure S4: (a) Elemental maps extracted from an EDX spectrum image at all tilt angles from -75° to 80°. (b) Elemental maps at -70°. (c) Normalized summed intensity of the elemental maps for the different elements at all acquired tilt angles.

S.7. Estimation of the influence of x-ray absorption

To estimate whether x-ray absorption has a significant impact on our results we calculated x-ray transmittivity for the materials present in our sample (Al, Si, Yb) at 1.5 keV, next to the x-ray line with the lowest energy used (Al-Kα: 1.49 keV). This can be done using the Beer-Lambert law for the transmittivity

$$T = {}^{I}/_{I_0} = e^{-\frac{\mu}{\rho}\rho d} \qquad \text{(Equation S1)}$$

μ/ρ is the mass absorption coefficient, ρ is the density and d is the x-ray path through the sample. We use an x-ray path of d = 113 nm, which corresponds to the maximum path an x-ray may have to traverse in a cylindrical sample with a diameter of 80 nm towards a detector positioned at an azimuthal angle of 45°. Table S1 shows mass absorption coefficients and densities for the materials present in our sample, results for the different materials (from[2]) and results for the transmittivity for the described worst case. For Al and Si 99% of the created x-ray can escape from the sample even in the assumed worse case. Even for the case of pure Yb 90% of the x-rays would still leave the sample. However Yb is present only in the form of local precipitates in the sample mixed with Al and Si, so in practice this worst case is far from being reached.

Material	**μ/ρ (cm^2/g) at 1.5 keV**	**ρ (g/cm^3)**	**$T = I/I_0$ (d = 113 nm at 1.5 keV)**
Al	402.2	2.699	0.99
Si	535.5	2.330	0.99
Yb	1350	6.730	0.90

Table S1: Mass absorption coefficient, density and calculated transmittivity

S.8. Tomographic reconstruction of elemental maps and spectral information

Reconstruction was done in MATLAB using 3D implementations for projection from the ASTRA tomography toolbox based on the graphics processing unit (GPU).[3] For the SIRT algorithm a multiplicative update was used for 30 iterations. Total-variation (TV) minimization reconstruction was done in MATLAB using the solver TVAL3[4] with projection and backprojection operators from the ASTRA toolbox. Pixel size of the image and spectrum images before reconstruction is 1 nm^2, which leads to a voxel size of 1 nm^3 in the reconstructions.

A comparison of using the 2D and 3D gradient for TV minimization is given in Fig. S5 for the example of the Si K-line elemental maps. Additionally also the impact of the weighting parameter μ is shown. The 3D algorithm links the different slices of the reconstruction in the y-direction and thereby removes stripe-like artifacts, perpendicular to the y-direction, which are visible when using the 2D algorithm. A small μ leads to stronger smoothing of the reconstruction and to less well defined interfaces between different regions. A large μ leads to smaller locally constant regions. If μ is chosen appropriately, regions with different elemental concentrations become well defined and sharp interfaces exist between the regions.

For the example of the Si K-line a weighting parameter of $\mu = 2^3$ was chosen. Similar tests were done for all EELS and EDX elemental maps to find suitable parameters for the algorithm.

Using 3D GPU based operators as compared to 2D operators, solving the 3D problem is even faster than solving a series of 2D problems, as the full capacity for parallel computation of the GPU can be utilized. In the present case the reconstruction from 32 elemental maps with a size of 194*156 pixels took about 5 minutes on a 64-bit system with an Intel Core i7-3820 quad core CPU, 64 GB RAM and an Nvidia GeForce GTX 670 GPU.

Reconstruction of EELS and EDS spectra is also done in MATLAB using GPU algorithms. Each spectral channel is treated as an independent tilt series and reconstructed using a multiplicative SIRT algorithm with 30 iteration. Focusing on the regions of interest in the spectra this requires 520 reconstructions for the low-loss spectrum (-10 eV to 250 eV, 0.5 eV/channel), 1600 reconstructions for the core-loss spectrum (1250 eV to 2050 eV, 0.5 eV/channel) and 800 reconstructions for the EDS spectrum (0 keV to 8 keV, 0.01 keV/channel). Reconstruction of each spectral channel with a SIRT algorithm takes about 15 s, the overall reconstruction time for all spectra was about 12 hours.

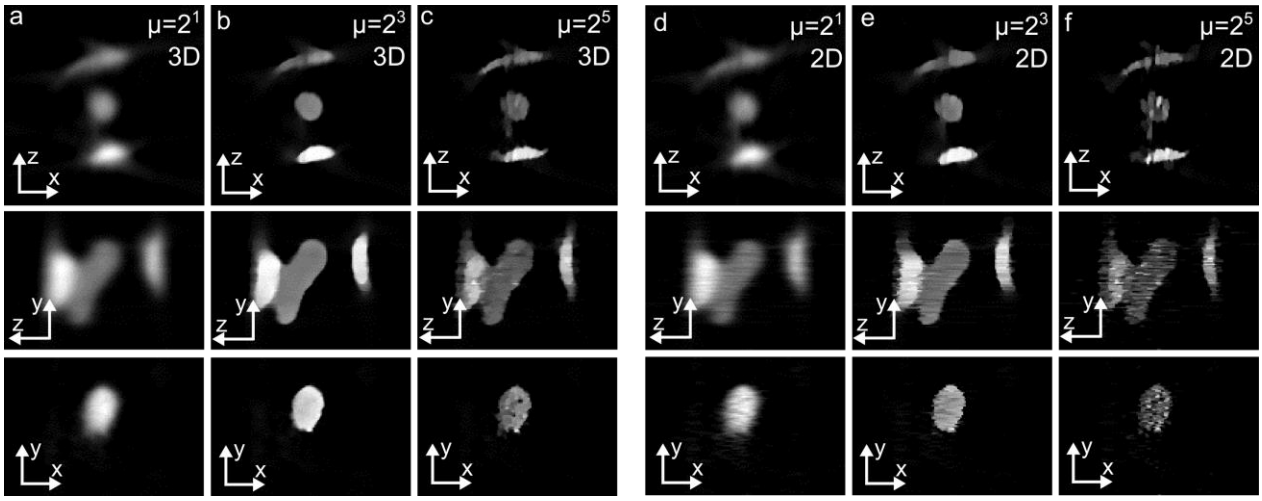

Figure S5: Comparison of 2D and 3D TV minimization algorithm and the effect of weighting parameter μ: (a-c) show orthogonal slices through a reconstruction with the 3D algorithm, (d-f) with the 2D algorithm. In (a) & (d) $\mu = 2^1$, in (b) & (e) $\mu = 2^3$, in (c) & (f) $\mu = 2^5$

S.9. Quantification of reconstructed spectra

We tested elemental quantification of reconstructed EELS and EDS spectra on spectra summed over Yb-rich precipates as shown in Fig. 5a in the main text. For quantification of EELS spectra we used model-based fitting using Hartree-Slater cross-section models for the absorption edges. We used two fit regions, a first region starting at 1250 eV up to 1850 eV, a second region starting at 1700 eV up to 1940 eV. The first region contains the Al K-edge and the Yb M_{45}-edge, the second region contains only the Si K-edge and ends just before the Yb M_3-edge. The spectrum as well as the model are shown in Fig. S6a. It can be seen that for the first fit region the model and the recorded spectrum do not match

well. The most likely reason for this mismatch is that the Hartree-Slater model does not describe the Yb M-edge well. In combination with the overlap of the Al K-edges and Yb M-edge this introduces errors in the quantification. Fig. S6b shows the spectrum and the model used for EDS quantification. Gaussian peaks are fitted at the positions of the different absorption lines together with a Kramers background model. For the EDS case sources of error are the overlap of Al K-lines and Yb M-lines, errors in the k-factors used for quantification. Quantification gave Al:Si:Yb compositions of at.% 43:47:10 in EELS and at% 48:35:16 for EDS.

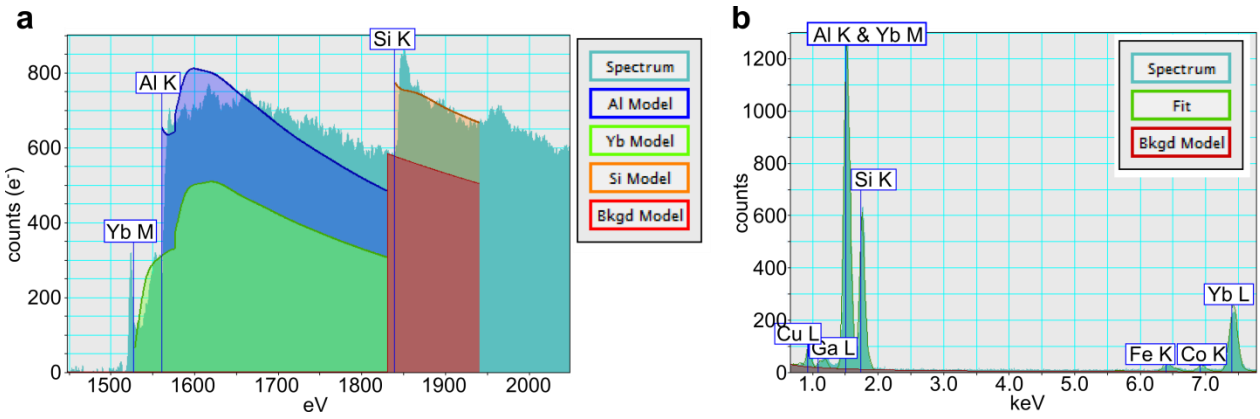

Figure S6: Setup for quantification of reconstructed spectra for (a) EELS spectrum, (b) EDS spectrum

References

1. F. de la Peña, M.-H. Berger, J.-F. Hochepied, F. Dynys, O. Stephan, and M. Walls, *Ultramicroscopy*, 2011, **111**, 169–176.
2. US Department of Commerce, NIST: X-Ray Mass Attenuation Coefficients http://www.nist.gov/pml/data/xraycoef/index.cfm (accessed Jun 26, 2014)..
3. W. J. Palenstijn, K. J. Batenburg, and J. Sijbers, *J. Struct. Biol.*, 2011, **176**, 250–253.
4. C. Li, W. Yin, H. Jiang, and Y. Zhang, *Comput. Optim. Appl.*, 2013, **56**, 507–530.